APPLICATION OF THE ESEM TECHNIQUE IN WOOD RESEARCH. PART II. COMPARISON OF OPERATIONAL MODES

Hrvoje Turkulin
Associate Professor
Faculty of Forestry, Zagreb University
Svetosimunska 25
10000 Zagreb, Croatia

Lorenz Holzer
Head of 3D-Mat group

Klaus Richter†
Head of Wood Laboratory
Empa, Swiss Federal Laboratories for Materials Testing and Research
Ueberlandstr. 129
8600 Duebendorf, Switzerland

and

Juergen Sell†
Professor, former Head of Wood Laboratory, Empa
Robaenkli 22
8607 Aathal-Seegraeben, Switzerland

(Received June 2004)

ABSTRACT

An ESEM (Environmental Scanning Electron Microscopy) technique has been applied to wood objects. ESEM investigations were performed through several operational modes that offer various sets of environmental and imaging conditions. The comparison of ESEM micrographs with conventional SEM images revealed specific advantages and shortcomings of the ESEM technique in studies on genuine and painted wood objects. Merits of the application of ESEM technique for wood are related to the absence of preparation artifacts, such as sputtering irregularities or defects due to shrinkage in vacuum drying. Great ESEM advantage over high-vacuum SEM, such as conduction of dynamic experiments within the chamber, is illustrated with a sequence of condensation, freezing, and drying on a wood specimen.

The wood imaging using ESEM proved inferior to that of conventional SEM in terms of lower magnification, sharpness, and contrast. However, the article offers guidance for assessment of influential operating parameters and their selection for the optimization of the ESEM work with wood. It may result in micrographs of sufficient resolution, definition, and optical quality for study of wood structure on cellular and even intra-cellular level.

Keywords: Wood, SEM, ESEM, wood structure, fractography.

INTRODUCTION

The first paper in a series (Turkulin et al. 2005) presented the basic operational parameters of the ESEM (Environmental Scanning Electron Microscope) technique in work with wood objects. Details on work with wood and a comprehensive literature survey are given in a more extensive ESEM research report (Turkulin et al. 2004). This paper aims at demonstrating the de-

† Member of SWST.

tails of specific wood experiments and comparisons of different operational ESEM modes with conventional SEM work.

The ESEM may be used in several operational modes, namely in *high vacuum* mode and three *environmental* modes. In *high vacuum* (HV) mode, the ESEM is used as a conventional SEM instrument with field-emission (FE) cathode. The chamber is highly evacuated, the specimens are almost absolutely dry and sputtered with a 10–15-mm-thick coating of gold or platinum (Zimmermann et al. 1994).

In *low vacuum* modes, the low pressures of water vapor are maintained within the chamber, and specimens with moisture content below fiber saturation point, usually below 15%, may be observed without drying or sputtering. *Low vacuum short distance* (LVSD) mode differs from the *low vacuum* (LV) mode in shorter working distances, shorter *beam gas path lengths* (BGPL), and higher pressures that could be applied, which all results in better imaging quality. The *Wet* mode (sometimes also called *ESEM* mode) is suitable for observation of wet or very moist objects under chamber vapor pressures usually in a range between 2 and 6 torr. Moistening, condensation, wetting, freezing, and thawing of the specimen, as well as heating and drying, can be established as dynamic processes within this mode during active imaging.

MATERIAL AND METHODS

Cross-sections of softwood specimens have been used for investigation, selected in two main groups: genuine wood in its natural appearance, and fragments of coated wood. Details of specimen preparation have been given previously (Turkulin et al. 2004, 2005); only general information is presented here. Three types of specimens were used in the study, namely thin strips, microtomed specimens, and fractured specimens of solid wood.

Thin strips of Scots pine (*Pinus sylvestris* L.) are 100-mm-long microtomed wood sections of radial block surfaces, used in studies of photodegradation (Derbyshire et al. 1995, 1996). The sections are 10 mm wide and 70 μm thick. The strips are conditioned (20°C, 65% RH) and tested for tensile strength. Their fractured cross-sections were subsequently microscopically analyzed in different operational modes.

Solid samples were taken from a painted pine window, and also prepared from a board of genuine spruce (*Picea abies* Karst.). Sticks 10 × 10 mm in cross-section were sawn from the bare or painted panels. Plane cross-sectional surfaces were prepared by microtoming wood in tangential direction on a sliding microtome. Some samples were subjected to "Wet microtoming," which refers to preparation after immersion of a sample in a mixture of equal volumes of water and ethanol for 30 min. Some of these specimens were used wet, others were dried naturally to obtain different moisture contents. "Moist" specimens were conditioned for 3 h at 20°C and 50% relative humidity. "Dry" samples were dried overnight in vacuum dryer at 20°C, and finally conditioned for 2 h in room conditions (20 ± 1°C, 55–60% RH) to approximate moisture content of 12%.

Fractured specimens of solid wood were prepared from 300-mm-long sticks. These sticks, 10 × 10 mm in cross-section, were tested in 3-point static bending, where the force was acting approximately in tangential direction. In the case of painted wood, the paint film surface was positioned in the tension zone. The tension zones of fractured ends were separated by a scalpel and either observed in ESEM in their natural appearance, or prepared for *high vacuum* mode microscopy. The latter included vacuum drying at 40°C for 24 h and standard sputtering with platinum for 25–30 s. All ESEM specimens were fastened to the mounting blocks using conductive carbon adhesive in such a way that adhesive extended for about 1 mm up the vertical sides of the sample.

The specimen for a dynamic trial of water condensation was made from a 10-× 10-× 300-mm stick cut from a spruce panel previously painted with the following exterior finishing system: isocyanate primer impregnation, waterborne acrylic basecoat, and two coats of acrylic top coat. It is estimated that the moisture content of the specimen was above 20%. The stick was

tested as described above, and a cube of approximate dimensions 4 × 4 × 4 mm was separated from the fractured portions. The specimen was glued with its paint surface to the L-shaped copper cold-stage holder, so that the heat flux was being transferred from a side to the paint layer. In this way a thermal gradient can be applied to the sample, by which the side of the paint layer is either cooled or heated, creating a front of condensation, evaporation, or sublimation.

RESULTS AND DISCUSSION

Comparison of different operational modes

Comparison low vacuum.–low vacuum short distance–ESEM mode.–Figure 1 presents a conventional, *high vacuum* (HV) mode micrograph of spruce cross-section. Imaging at low magnifications in *low vacuum* mode (Fig. 2) does not show great differences to HV micrograph. The *low vacuum short distance* mode gave the best results on conditioned wood (up to 12% MC) in a range of magnifications up to 5000× (Fig. 3a). Direct comparison of Fig. 3a and 3b clearly shows that *Wet* mode yields lower resolution and more pronounced edge effect than *LVSD* mode, obviously due to higher vapor pressures. At pressures below 4 torr in *Wet* mode, the contrast is very low.

Low vacuum mode is more practical than the *low vacuum short distance* mode, since the field of observation is much broader. However, *low vacuum short distance* mode offers a wider range of vapor pressures, the beam gas path length (BGPL) is shorter, and consequently the overall quality of the image can be optimized more efficiently than in a *low vacuum* mode (compare Fig. 3a and Fig. 2).

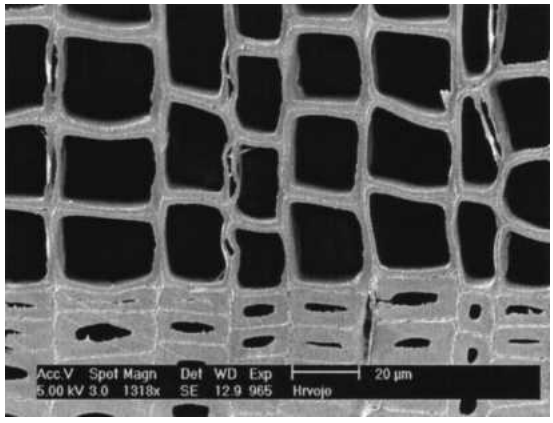

FIG. 1. Uncoated spruce, microtomed in wet (saturated) condition, and subsequently dried. *High vacuum* (HV) mode, platinum sputtered. Mag. ca 1300×.

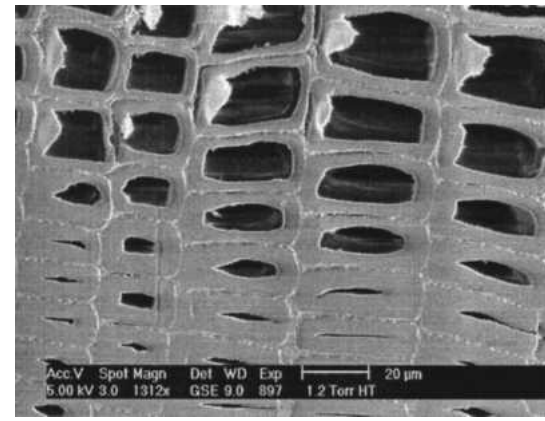

FIG. 2. Uncoated spruce, microtomed in wet (saturated) condition. *Low vacuum* (LV) mode. Mag. ca 1300×.

Comparison low vac short distance-high vacuum mode.—In an attempt to record the same detail in *low vacuum short distance* mode and *high vacuum* modes, a particular specimen was first observed in LVSD mode without drying and coating (Figs. 3a and 4a). The specimen was then prepared for observation in high vacuum: it was vacuum dried, sputtered with platinum, and observed in HV mode of the ESEM (Figs. 1 and 4b). Comparison of Figs. 1 and 3a shows that the quality of LVSD images at lower magnifications is not significantly lower than that of HV images.

The image on Fig. 4b does not show any widening of the cracks due to drying and contraction in conditions of high vacuum operation. On the contrary, some of the voids between the cells, in the region of the compound middle lamella (CML), seem to be smaller in HV image, with peculiar filling of the lumen of the central latewood cell (arrow). The depth resolution of an LVSD mode was shown previously to be sufficient for covering the topographic depth greater than 2–3 μm. The filling in the lumen should

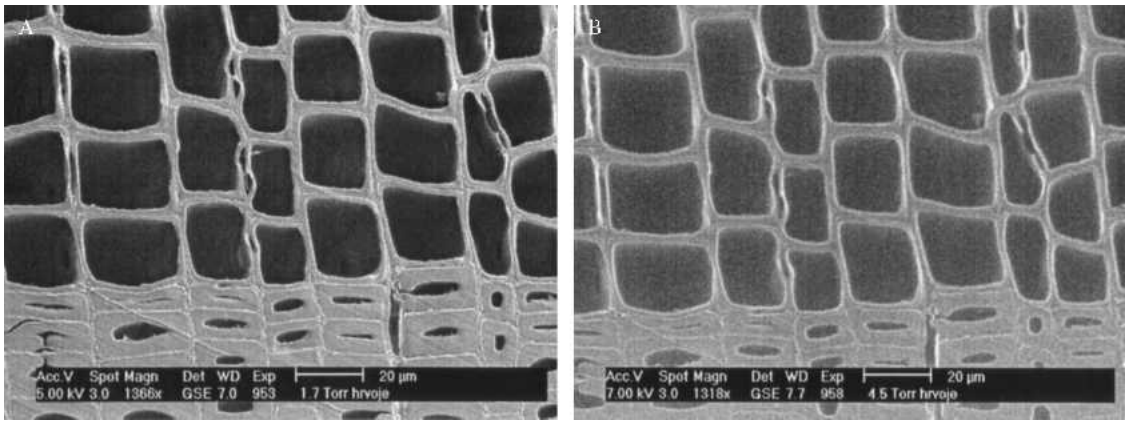

FIG. 3. Transverse surface of spruce, microtomed in wet (saturated) condition. Mag. ca 1300×. Left: *Low vac short distance* (LVSD) mode, 5 kV, and 1.7 torr (3a). Right: *Wet* (*ESEM*) mode, 7 kV and 4.5 torr (3b).

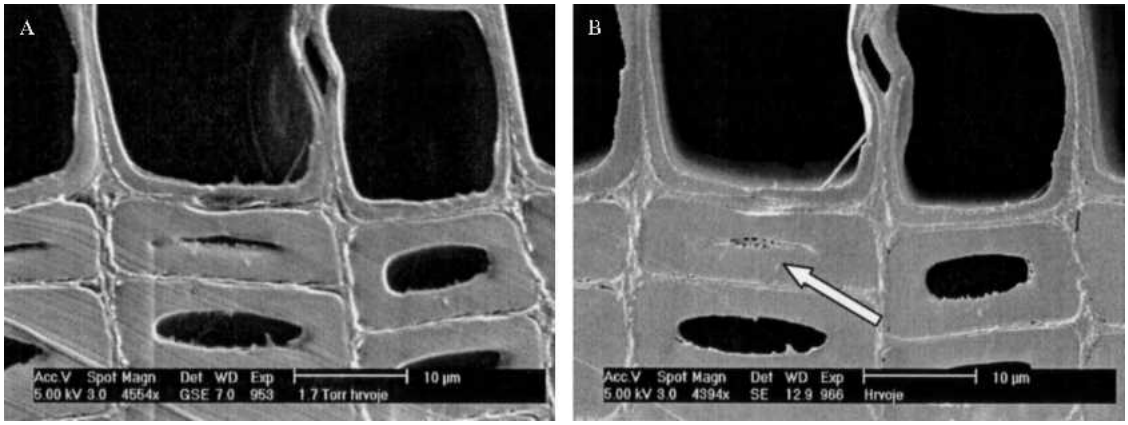

FIG. 4. Transverse surface of spruce, microtomed in wet (saturated) condition. Mag. ca 4400×. *Low vacuum short distance mode*, 5 kV, 7 mm WD, and 1.7 torr pressure (left). *High vacuum* mode, 5 kV, platinum-sputtered sample (right). Arrows indicate platinum deposit after drying and sputtering of the same specimen for observation in HV mode.

therefore also be clearly observable on the LVSD image (Fig. 4a), which is not the case. This illustrates a typical preparation defect that may happen in high vacuum microscopy, manifested as a platinum deposit, which may cover details of the real specimen surface. A usual procedure for conventional platinum sputtering, using voltages of 400–700 V and 50–60 mA during 25–35 s, leads to a typical coating thickness of approximately 15 nm (Zimmermann et al. 1994). It is possible, however, that the unevenness of conductivity of the specimen causes excessive deposit of coating.

A direct comparison of the same detail of a fractured thin strip on pairs of images on Figs. 5 and 6 enables a good insight into possible damage that may be caused to the specimen by the preparation procedure for the observation in an HV mode. Drying defects are almost invisible at low magnifications (Fig. 5). However, comparison of LVSD and *high vacuum* images at higher magnification (>6000×, Fig. 6) clearly shows that some changes (shrinkage and deformation) have occurred during vacuum drying and sputtering.

The upper left cell-wall segment is more twisted inwards on Fig. 6b than on Fig. 6a. The connecting fibrils between that cell-wall seg-

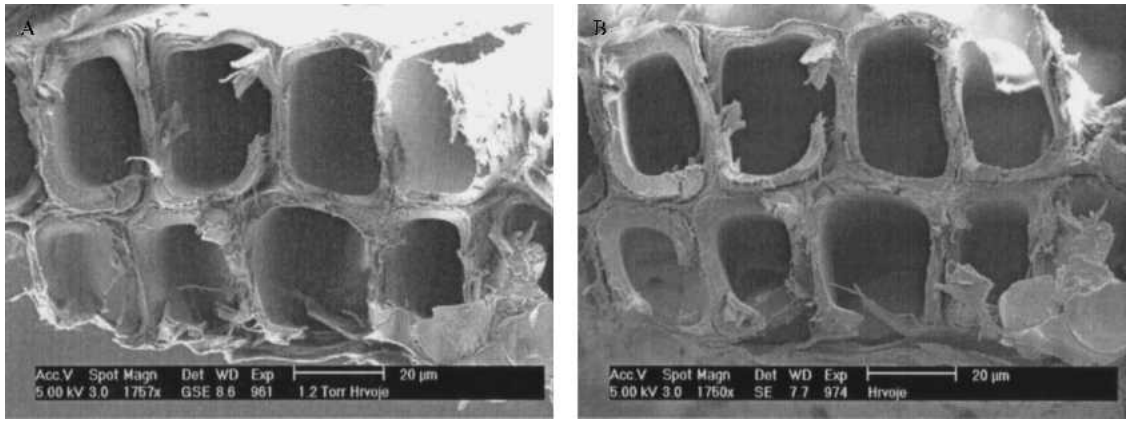

FIG. 5. Unweathered thin strip of Scots pine sapwood, failed in tension. **Left:** *Low vacuum short distance mode*, genuine wood. **Right:** *High vacuum* mode, platinum-sputtered wood. At low magnifications LVSD and HV mode do not show great differences.

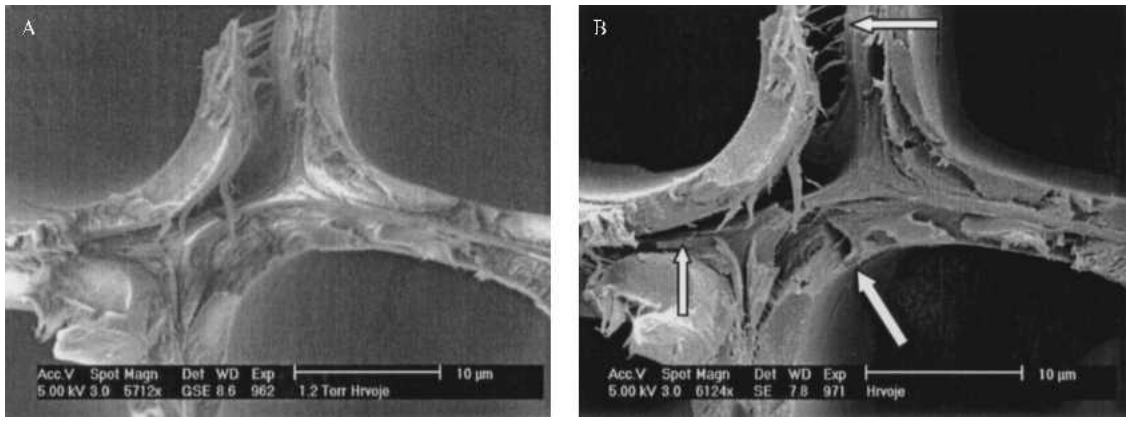

FIG. 6. Walls of softwood earlywood tracheids at their corner joint (details from Figs. 5a and b, respectively, mag. ca 6000×). Both images are taken at 5 kV acc. voltage and at similar working distance. Left: *Low vacuum short distance* mode, genuine wood. Right: *High vacuum* mode, platinum-sputtered wood. Arrows indicate the enlargement of existing cracks and opening of new ones as a consequence of vacuum-drying.

ment and the CML are either broken or missing on an HV image (upper arrow). Some cracks have enlarged due to the shrinkage on Fig. 6b (arrows). There are cracks that appear smaller on the LVSD image due to obvious insensitivity of the low vacuum technique to record details with great resolution. However, all the important details, precisely recorded in an HV mode, are also discernible in the LVSD mode.

In summary, the damage due to shrinking can be documented, but in this case no notable new artifacts occurred in the preparation for the HV observation. It should be mentioned that the intensity of shrinkage defects presented here is relatively small because the comparison was being made between already conditioned wood (≈12%) and vacuum dried wood. When wood would be observed in saturated state and subsequently thoroughly dried, the shrinkage would cause much greater consequences, which is also well documented by Gu et al. (2001). Furthermore, the specimen on Figs. 5 and 6 was only about 70 μm thick, and shrinkage constraints of such small wood objects are much lower than

Gu's solid wood specimens of larger dimensions (6 × 6 × 6 mm).

Pairs of micrographs on Figs. 5 and 6, performed in a *low vacuum short distance* mode and *high vacuum* mode, show the fractured cross-section of a Scots pine thin strip. This motive was frequently explored in previous research as it enables a delicate surface of a tension-failed cross-section of wood cells to be examined (Zimmermann et al. 1994; Zimmermann and Sell 1997; Turkulin and Sell 1997, 2002). A tough, interlocked failure mode could be seen here, showing pulled-out fibrils, torn bundles, and radial agglomerations of fibrils (structures of the S2 layer perpendicular to the middle lamella). Smooth portions of the cell-wall cross-sections indicate portions of the rapid crack development, delamination of compound middle lamella, or the separation of the cell-wall layers.

The images taken in LVSD mode offer a good general insight into the fractographic appearance of the softwood latewood tissue. LVSD images depict the main characteristics of the fractured tracheids: delamination due to fracture stresses, cracks partly bridged by single fibrils, and voids from pulled-off bundles of fibrils and fragments of cell wall. Larger magnification of the detail (Fig. 6a) enables sufficient contrasting and resolution of the minute details of the cell-wall structure.

The observations lead to the following conclusions:

- *High vacuum* mode
  - —offers significantly better resolution, contrasting, and depth resolution on wood than LVSD mode.
  - —causes shrinkage and distortions due to drying stresses; a risk of irregular or excessive metal deposit in sputtering is also present. The relative significance of these effects need not be detrimental for the analysis, but must be carefully evaluated for each particular specimen.
- *Low vacuum short distance* mode
  - —shows sufficient resolution and imaging quality for investigations of wood at magnifications up to 5000×.
  - —enables specifically the general structure of the cell wall and the fractured surface to be studied without extensive drying.
  - —offers great saving of time in sample preparation.

Condensation experiments in Wet mode

An example of dynamic processes that could be simulated within the chamber using the *Wet* mode are condensation–drying cycles induced in the studies of wet adhesion. Adhesion loss between the exterior coating and the wood surface was found to be one of the major causes of paint failure in exterior applications (Turkulin et al. 2002).

Microscopic analysis of the adhesion-tested specimens revealed that failures often happen either in the weak substrate, or in the base-coat layer. The base-coat is often found to be porous and brittle due to a high pigment concentration (Fig. 7a). The ingress of water into these microvoids (Fig. 7b) possibly contributes to the swelling and loss of cohesive strength of the base-coat.

Figures 8a to f present a sequence of events recorded during temperature changes within a −5°C to +55°C range using a cooling (Peltier) stage. The intention of such an experiment was to provoke condensation at the wood-paint interface and monitor the infiltration of water into the interface voids. The sample is cooled and heated via a metal piece at the contact with the painted wood (top of image). In this way, temperature gradients and a corresponding condensation/drying front can be invoked.

Figure 8a shows that the paint layer exhibits different properties than wood in interaction with the electrons, since it appears brighter on the image. Temperature of the stage was 11.2°C. When the cooling stage was activated with a target temperature of −0.3°C, the paint surface was cooled to 4.2°C in nearly 2 min. However, no changes on the specimen were observed until the pressure was increased to 5.6 torr. At that point, condensation started swiftly, and Fig. 8b was scanned. Glow on a paint surface indicates that water molecules condensed on the paint

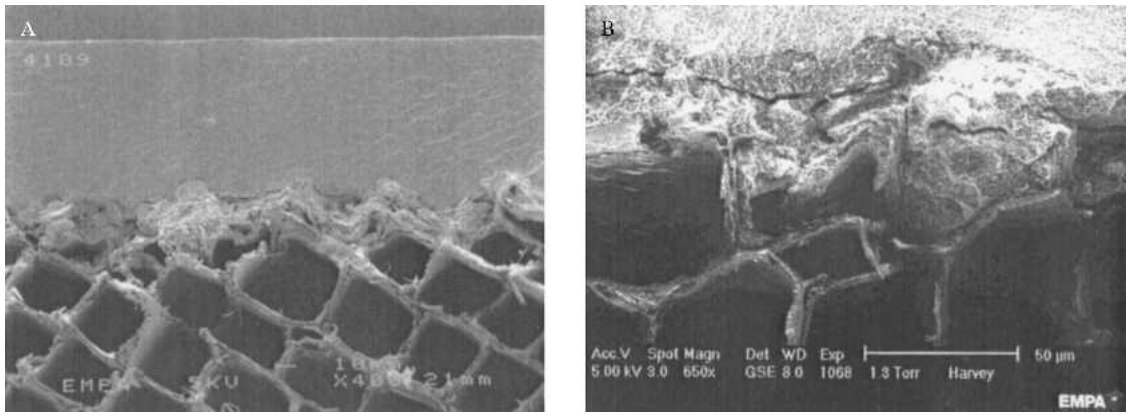

FIG. 7. HV mode (7a, left) and *Wet* mode (7b, right): Fractured end-grain surface of spruce earlywood impregnated with isocyanate primer and painted with an opaque system. Two topcoats of acrylic paint coalesced in a homogenous, tough layer (left). Pigment-rich base coat looks brash and brittle, with a lot of micro-voids for possible water ingress and loss of cohesive strength (right).

layer quickly, while wood (less conductive) was not cooled down so rapidly due to the asymmetric contact with the cooling stage.

Maintaining the vapor pressure at 5.3 torr and lowering the temperature to 2.1°C caused intensive condensation on the paint layer and on adjacent wood cell walls (Fig. 8c). As the film of water molecules accumulated over the entire surface (Fig. 8d), the brightness of the paint and the wood equalized, reducing the contrast between the two layers.

The change of the target temperature to −12°C caused intensive cooling of the paint, and after ca 2 min, the water on the specimen swiftly, within seconds, turned to ice (Fig. 8e). The vapor pressure was then lowered to 2 torr to avoid growth of ice crystals on the surface.

A reverse process, the heating of the specimen (thawing and subsequent drying), occurred after sudden change of the target temperature to +40°C. The temperature increased to +4.5°C and remained so for nearly 3 min, while a large amount of water was evaporated. That caused rapid changes in automatic step-wise adaptation to maintain the target chamber pressure of 3.1 torr, and an image with steady conditions could not be taken. Only after removal of the surface water and heating up to 25°C for 5 min, the conditions stabilized. Conditioning at reduced temperature (12°C) lasted about 7 min, and the final scan was made (Fig. 8 f) under the same conditions as at the beginning of the sequence (Fig. 8a).

Some deformations of the thermoplastic paint fragments can be seen in the interface cells (compare with Figs. 8a and 8f). Although some changes are notable, no substantial enlargement of the voids in the porous layer that could be attributed to the effect of moistening, freezing, and drying stresses can be seen. Repeated sequence might result in greater changes of the specimen due to swelling, freezing, and drying, but caution should be taken to avoid the beam damage.

CONCLUSIONS

ESEM offers various environmental operational modes, in which pressures of water vapor up to 10 torr can be maintained within the chamber. Thus, samples retain their initial moisture content. Results from the different ESEM modes were compared with high vacuum imaging of classical SEM.

Low vacuum mode offers wider field of observation than *low vacuum short distance* mode. LVSD mode, on the other hand, offers a larger range of vapor pressures and better overall quality of the images. LVSD mode gives the best results on conditioned and non-sputtered wood

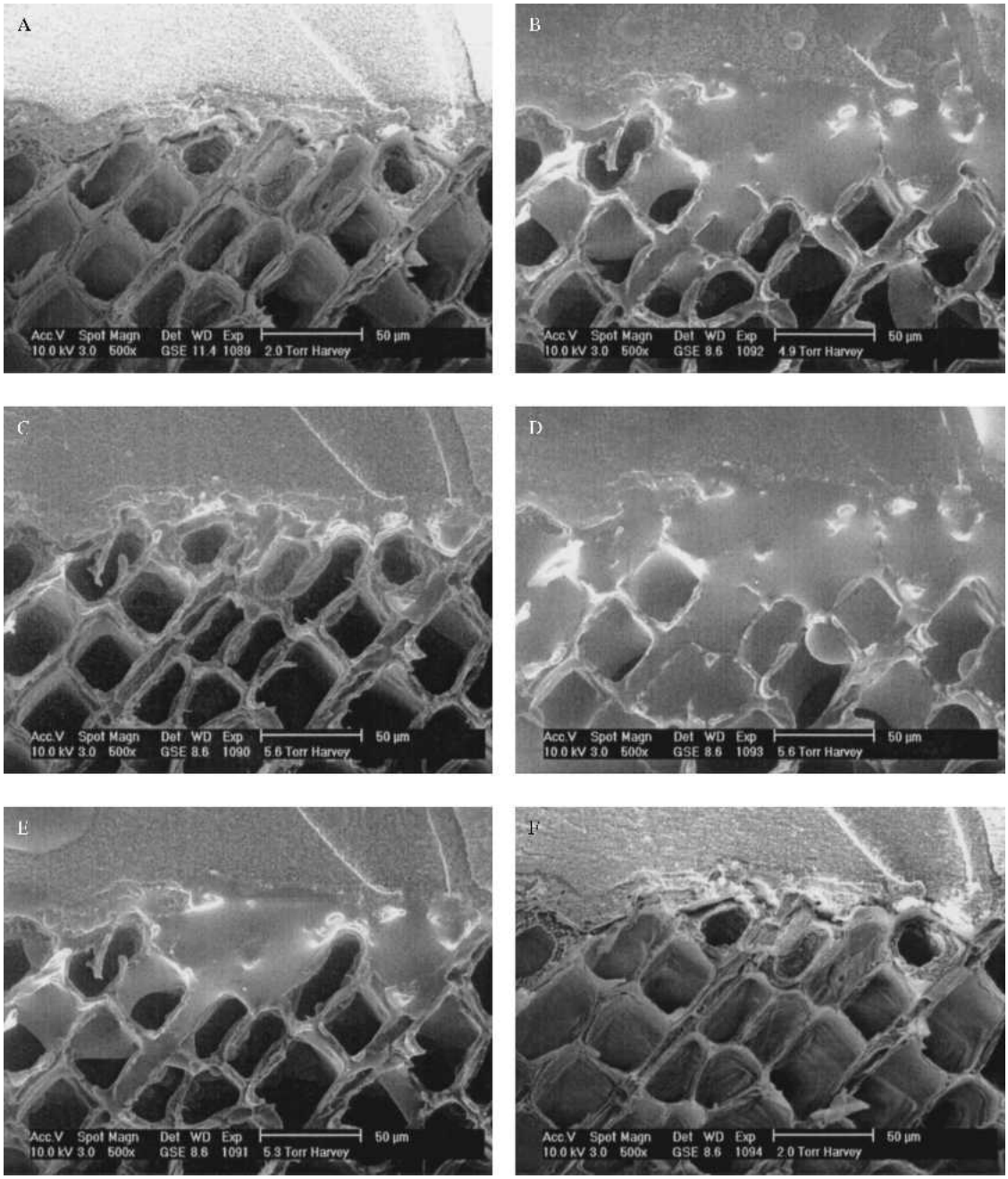

FIG. 8. Descending: a, b, and c in left column, d, e, and f in right column: Interface of the painted spruce wood, subjected to cooling (a,b,c), condensation (b,c,d), freezing (e) and sublimation-drying (f) in *Wet* mode. In order to invoke temperature gradients, the sample was cooled asymmetrically using a special geometry of the cooling stage. The metal piece in contact with the peltier cooling stage was attached at the top of the images, i.e. in contact with the painted surface.

and should be applied if the quality images are required in a range of magnification between 800 and 5000×.

As in conventional SEM, a *high vacuum* mode of ESEM ensures significantly better resolution, contrast, and depth resolution than LVSD mode. However, it was shown to cause shrinkage and distortions due to drying stresses, and a risk of irregular or excessive metal deposit during sputtering.

The general fractographic analysis may be almost equally well performed in LVSD and in HV modes. The preparation of specimens for LVSD mode would be advantageous in terms of shorter time requirements and the absence of artifacts related to vacuum-drying and sputtering.

Wet mode yields lower resolution and stronger edge effect than *LVSD* mode, but is indispensable in observation of very moist or wet wood objects. Dynamic physical processes that could be performed within the chamber in the *Wet* mode, such as condensation, freezing, drying and heating, underline the great potential of the ESEM microscopic technique in research on wood and similar materials.

REFERENCES

DERBYSHIRE, H., E. R. MILLER, AND H. TURKULIN. 1995. Investigations into the photodegradation of wood using microtensile testing. Part 1: The application of microtensile testing to measurement of photodegradation rates. Holz Roh-Werkst. 53(4):339–345.

———, ———, ———, 1996. Investigations into the photodegradation of wood using microtensile testing. Part 2: An investigation of the changes in tensile strength of different softwood species during natural weathering. Holz Roh-Werkst. 54(1):1–6.

GU, H-M., A. ZINK-SHARP, AND J. SELL. 2001. Hypothesis on the role of cell wall structure in differential transverse shrinkage of wood. Holz Roh-Werkst. 59:436–442.

TURKULIN, H., AND J. SELL. 1997. Structural and fractographic study on weathered wood. An application of FE SEM microscopy to the "Thin strip" method. Research and work report No. 115/36. Swiss Federal Laboratories for Materials Testing and Research (EMPA). Dübendorf, Switzerland. 40 pp.

———, AND ———. 2002. Investigations into the photodegradation of wood using microtensile testing. Part 4: Tensile properties and fractography of weathered wood. Holz Roh-Werkst. 60(2):96–105.

———, K. RICHTER, AND J. SELL. 2002. Adhesion of waterborne acrylic and hybrid paint on wood treated with primers. Surface Coatings Internat. Part B: Coatings Transactions Vo. 85, B4, 273–280.

———, L. HOLZER, AND J. SELL. 2004. Application of the ESEM technique in wood research. Research and work report No. 115/51. Swiss Federal Laboratories for Materials Testing and Research (EMPA), Dübendorf, Switzerland. 58 pp.

———, ———, K. RICHTER, AND J. SELL. 2005. Application of the ESEM technique in wood research. Part 1: Optimization of imaging parameters and working conditions. Wood Fiber Sci. (in press).

ZIMMERMANN, T., AND J. SELL. 1997. Die Feingefüge der Zellwand auf Querbruchflächen von längszugbeanspruchten Laubhölzern. Research and work report No. 115/35. Swiss Federal laboratories for Materials Testing and Research (EMPA), Dübendorf, Switzerland. 37 pp.

———, ———, AND D. ECKSTEIN. 1994. Rasterelektronenmikroskopische Untersuchungen an Zugbruchflächen von Fichtenholz. Holz Roh-Werkst. 53(4):223–229.